Program Digest, 2019 IEEE International Ultrasonics Symposium (IUS)
Glasgow, Scotland, October 6-9, 2019

ScAlN polarization inverted resonators and enhancement of k_t^2 in new YbAlN materials for BAW devices.

Takahiko Yanagitani[1,2,3] and Junjun Jia [1]
[1] *Faculty of Science and Engineering Waseda University, Tokyo, Japan,* [2]*ZAIKEN, Japan,* [3]*JST-PRESTO, Japan*
Email : [1] yanagitani@waseda.jp

***Abstract*—AlN thin piezoelectric films are attractive for RF filter applications because of their low mechanical loss $1/Q_m$. We here introduce new AlN based materials: polarization inverted ScAlN multilayer and YbAlN films. These materials are promising for application in BAW and SAW devices.**

Keywords—Polarization inverted layer; AlN; ScAlN; YbAlN; BAW resonators

I. INTRODUCTION

Polarization-inverted multi-layer structure is attractive for thin film resonator, SAW device, ultrasonic microscope, and non-linear optics applications. Here, the growth method of the structure for AlN, ScAlN, and ZnO films are introduced. We also demonstrate the performance of the overtone mode resonators consisting of the polarization-inverted multi-layer.

In the RF acoustic filter applications, both high electromechanical coupling k_t^2 and low mechanical loss $1/Q_m$ are required. Therefore, low loss AlN films are used in the BAW filters in spite of their low k_t^2. ScAlN films [1] are attracting interest as BAW [2] and SAW devices because of their high k_t^2 [2]. We also report the discovery of new doping of Yb as an alternative element to the Sc [3].

A. Thin film resonator application

A resonator with single piezoelectric layer excites fundamental (1st) mode resonance. In contrast, *n*th polarization inverted multilayer film resonator excites *n*th high overtone mode resonance. Therefore, the resonant frequency in *n*th polarization inverted film resonator is *n* times higher than that of single piezoelectric layer resonator when both films have equal thickness. On the other hand, in the same operating frequency, polarization inverted multilayer make it possible to increase their film thickness. This contributes to the rigidity of the device and the high power handling capability.

It is well known that the energy trapping mode cannot occur when ratio of longitudinal wave and shear wave velocities $(c_{33}^D/c_{44}^E)^{1/2}$ in the piezoelectric plate is smaller than 2 [4]. Thickness extensional mode (TE) in ZnO film have energy trapping mode because the ratio $(c_{33}^D/c_{44}^E)^{1/2} = 2.33$ exceeds 2. In contrast, TE energy trapping mode cannot be used in the AlN and $Sc_{0.41}Al_{0.59}N$ films in standard electrode configuration because the ratio of AlN and $Sc_{0.41}Al_{0.59}N$ are 1.75 and 1.51, respectively [5]. On the other hand, Kittaka et al. proved that 2nd overtone TE mode in polarization inverted $PbTiO_3$ structure have energy trapping mode although the ratio in $PbTiO_3$ is 1.91[6]. It is expected that overtone TE mode in polarization inverted AlN and ScAlN multilayer also have energy trapping mode.

Nakamura et al. reported 60 MHz 2nd overtone TE mode resonator in domain inverted $LiNbO_3$ plate [7]. Larson et al. recently reported 2nd overtone TE mode FBAR consisting of polarization inverted c-axis oriented AlN films [8].

B. SAW device application

Effective electromechanical coupling coefficient of layered structure for SAW determines the band width of the filter. We here compare the coupling of the conventional single piezoelectric layer/non-piezoelectric substrate structure and new polarization inverted piezoelectric layer/non-piezoelectric substrate structure. We demonstrate the enhancement of the coupling by using polarization inverted structure.

C. Ultrasonic microscope application

In the un-tuned transducer, larger thickness (low capacitance) of the piezoelectric layer leads larger transducer area in order to obtain impedance matching between the transducer and the 50 Ω measurement system. *n*-Fold larger film thickness in the *n*-times polarity inverted transducer gives the *n*-times increase of transducer area. In the ultrasonic microscope application, this large transducer area (large emission area) directly contributes to the increase of acoustic pressure in the focus point as shown in Fig. 1 (a) and (b).

D. Nonlinear optics application

The commonly used $LiNbO_3$ and GaAs nonlinear optical (NLO) crystals are non-transparent in the ultraviolet and far-infrared regions. AlN possess high nonlinear optical coefficient and transparency in these regions. Therefore AlN are promising for laser wavelength conversion applications [9,10]. A spatially periodic polarity-inverted film structure, as shown in Fig. 2 (d), is required for waveguide-type quasi-phase matching NLO devices [11-13] because the maximum intensity of the second harmonic generation (SHG) appears when the c-axis is parallel to the *E*-vector of the incident light. Conversely, the SHG intensity goes to zero when the c-axis is perpendicular to the *E*-vector [14].

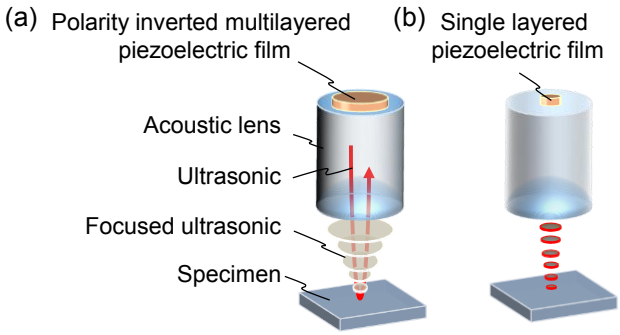

Fig. 1. Concentration of the ultrasonic in the ultraosonic microscope. Large transducer area (large emission area) directly contributes to the increase of acoustic pressure in the focus point.

II. Polalization Invertion of (0001) AlN and ScAlN Films

A. Film growth

c-axis oriented AlN film can be classified as either an (000-1) N-polarity shown in Fig. 2 (a) or an (0001) Al-polarity shown in Fig. 2 (b). The insertion of a buffer layer is one of the approaches to control polarization direction in III-nitride film growth [8,15,16]. AlN epitaxial buffer layer between a (0001) GaN layer and an Al_2O_3 substrate leads the unusual polarity inversion of the epitaxial GaN layer [15]. Larson et al. reported the polarization control of a (0001) AlN film by using clean Al under-layer [8]. Milyutina et al. showed the polarization-inverted growth of the sputter-deposited AlN film by using thin MOCVD AlN buffer layer [16]. However, the multilayer polarization-inverted structure, such as that shown in Fig. 2 (c) cannot be obtained by these polarization inversion techniques using buffer layer surface because the polarity of the second and subsequent layers cannot be controlled. Polarization inversion without using the buffer layer makes it possible to obtain polarity-inverted multilayer structure as show in Fig. 2 (c).

Akiyama et al. reported the polarization inversion of an AlN film by introducing a small amount of O_2 gas to the sputtering gas [17] or by increasing the cathode RF sputtering power [18]. They explained that the polarization inversion was caused by increasing the amount of pure Al particles around the substrate, based on the prediction of Al-polar film growth in Al-rich conditions by first principles calculations [19]. However, the mechanism of this polarization-inverted film growth was unclear.

On the other hand, we previously investigated the development of unusual a-axis (c-axis parallel) oriented wurtzite films by ion beam irradiation during film growth [20, 21]. We explained that this was caused by the ion beam tolerant (or sputtering yield) anisotropy of wurtzite crystal. Similarly, we assumed that the polarization inversion of wurtzite films is induced by ion beam tolerant anisotropy between (0001) and (000-1) planes. On the basis of this assumption, the effect of ion beam irradiation on the polarization of c-axis oriented wurtzite ScAlN films was investigated.

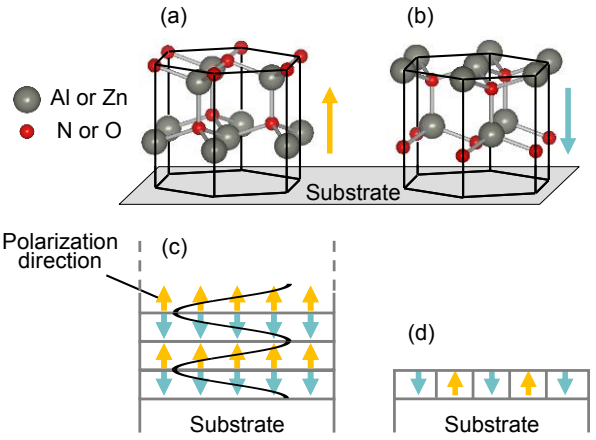

Fig. 2. (a) N-polar (000-1) AlN film or O-polar (000-1) ZnO film, (b) Al-polar (0001) AlN film or Zn-polar (0001) ZnO film, (c) polarization inverted multilayered structure, and (d) periodically polaization inverted structure.

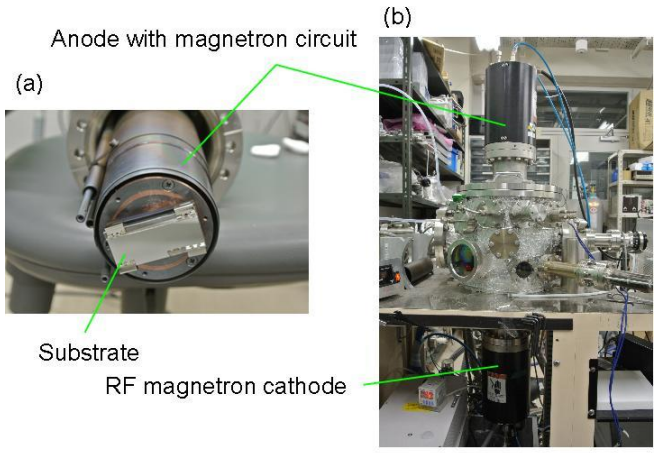

Fig. 3. Images of (a) the substrate and (b) the apparatus for RF bias sputtering deposition

c-axis oriented AlN and $Sc_{0.2}Al_{0.8}N$ films were grown by anode RF bias sputtering deposition as shown in Fig. 3 (b). Ion beam irradiation during the film growth can be enhanced by applying an RF bias to the substrate [22]. The substrate was set on an anode with magnetron circuit, and 14 MHz RF bias at 0.5 W was applied to the substrate as shown in Fig. 3 (a). (0001) oriented Ti electrode film (rocking curve FWHM value = 4.0 — 4.6°) on silica glass was used as the substrate. For comparison, AlN film was grown using the condition which is close to the commonly-used AlN film growth condition. In this condition, the enhancement of the ion beam irradiation by the magnetic fields of magnetron circuit was suppressed by covering the anode with an iron plate.

B. Determination of polarization direction

The polarity of the AlN films was determined by a press test [23]. A Cu top electrode (100 nm) was evaporated onto the films, and a compressive stress was applied to the top electrode by a probe (U1560A, Agilent Technologies) to measure the piezoelectric response of the films using an

oscilloscope (U1604A, Agilent Technologies). The polarity of the films was determined from the sign of the piezoelectric response. In addition, c-plane ZnO single crystal (Tokyo Denpa Co., Ltd., 10×10×0.5 mm^3, $>10^{10}$ Ω·m) was prepared as a reference sample for the press test. When the compressive stress was applied, a negative or a positive amplitude response appeared in the Zn-polar or O-polar ZnO single crystal, respectively, as shown in Figs. 4 (a).

As shown in Fig. 4 (b), when the compressive stress was applied, a negative response, indicating Al-polarity, were observed in the film grown using the condition which is close to the commonly-used AlN film growth condition (RF substrate bias =0.00W). In contrast, a positive response, indicating N-polarity, were observed in the film grown with an RF bias of 0.50 W. These results demonstrate that the polarity of the AlN film is inverted from Al-polarity to N-polarity by enhancing ion beam irradiation during the film growth. As previously assumed, the polarization inversion by ion beam irradiation may result from ion beam tolerant anisotropy between N-polar (000-1) and Al-polar (0001) crystal planes. We deduced that Al-polar (0001) oriented crystal growth is inhibited by ion beam irradiation, and relatively damage tolerant N-polar (000-1) oriented crystals develop preferentially. Detailed results of the various substrate bias wattage were described in the literature [24].

It is also well-known that the ion beam irradiation during film growth induces the stress in the film. Actually, we found that the crack must appear at the surface of all N-polar film. In contrast, the smooth surface was formed in all Al-polar films. From these results, in addition to the ion beam tolerant anisotropy, the stress in the films also may relate to the mechanism of this polarization inversion by ion beam irradiation [24].

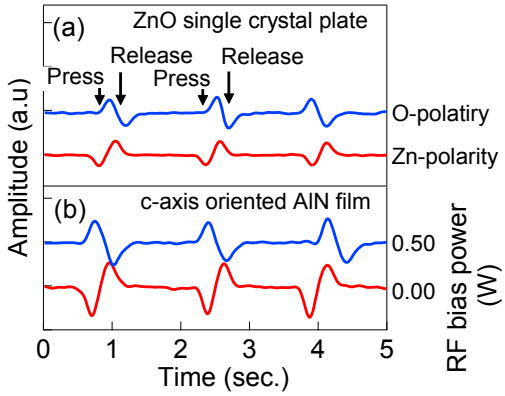

Fig. 4. Piezoelectric responses of (a) ZnO single crystal plate as a reference and (b) the response of AlN films grown with and without an substrate RF bias. Al-polarity and N-polarity are indicated as red lines and blue lines, respectively.

C. *Polarization inverted ScAlN FBAR*

Fig. 5 shows the frequency response of admittance in the polarization inverted two-layer $Sc_{0.2}Al_{0.8}N$ FBAR fabricated by using RF bias sputtering technique [25]. Also shown is the admittance single layer ScAlN FBAR where the entire film thickness is equal to the polarization inverted two-layer FBAR. In comparison with the monolayer FBAR, we can see second overtone mode excitation with suppression of fundamental mode and 3rd mode in the two-layer FBAR. This result demonstrates the complete polarization inversion in the two-layer FBAR [25].

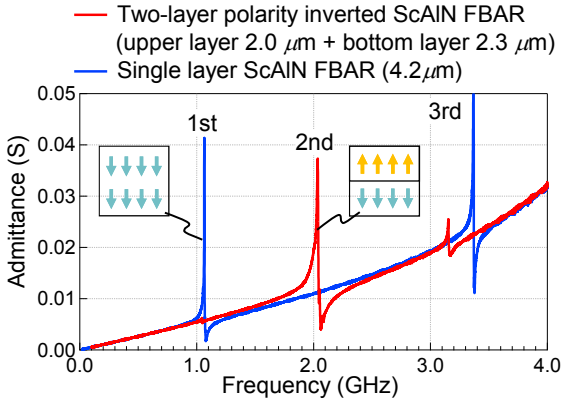

Fig. 5. Experimental frequecny responses of the admittance of (a) single layer $Sc_{0.2}Al_{0.8}N$ FBAR and two layer polarization inverted $Sc_{0.2}Al_{0.8}N$ FBAR. Note that both resonator have equal film thickness.

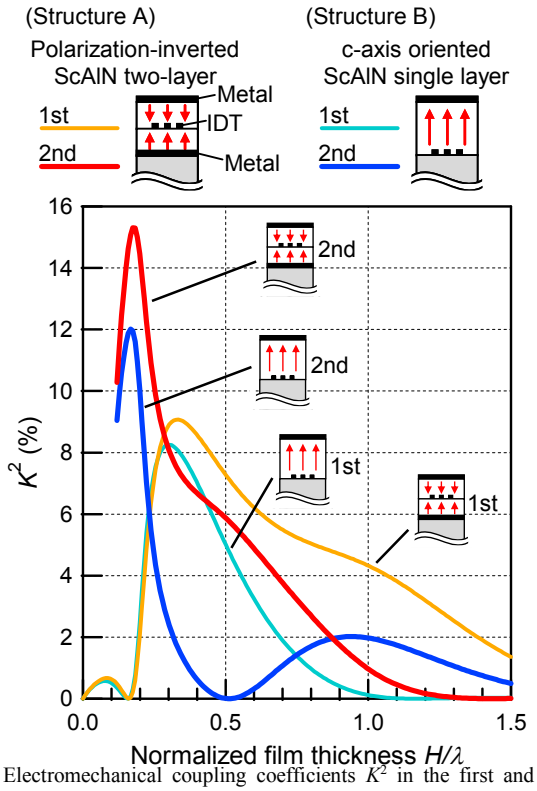

Fig. 6. Electromechanical coupling coefficients K^2 in the first and second mode Rayleigh-SAWs with polarization-inverted (0001)/(000-1) $Sc_{0.4}Al_{0.6}N$ two-layer/diamond and (0001) $Sc_{0.4}Al_{0.6}N$ single layer/diamond.

D. *SAW properties of polarization inverted ScAlN films*

To investigate the advantage of new polarization inverted structure for the SAW application, propagation characteristics of SAWs in the polarization-inverted (0001)/(000-1) $Sc_{0.4}Al_{0.6}N$ two-layer on a diamond substrate were

theoretically analyzed. The physical constants of ScAlN predicted by density functional theory [26] were used in the analysis. The both layer thicknesses were same in the analyses. Fig. 6 shows the calculation results of electromechanical coupling coefficients K^2 as a function of normalized film thickness H/λ. Maximum K^2 values were found to be 9.1% at $H/\lambda = 0.33$ (phase velocity: $V = 5940$ m/s) in the first mode Rayleigh-SAW and 15.3% at $H/\lambda = 0.18$ ($V = 10240$ m/s) in the second mode Rayleigh-SAW. K^2 values with the conventional (0001) $Sc_{0.4}Al_{0.6}N$ single layer on a diamond substrate were also calculated. Compared with the results of the single layer, high K^2 values were obtained in the polarization-inverted two-layer, especially in the second mode Rayleigh-SAW propagating at the boundary of the two-layer.

III. Polalization Invertion of (0001) ZnO Films

A. *Film growth*

Polarization inverted film growth can be also achieved in the c-axis oriented ZnO film. In the oxide sputtering growth, high energetic negative ion is generates at oxide sputtering target, due to their high electronic affinity, and bombards to the substrate. Therefore, ion irradiation in the substrate naturally occurs in the oxide sputtering growth and we do not need RF anode bias to induce unusual polarization inversion film growth. Our group knows experientially that ion beam induced unusual crystal growth occurs only in the condition of low film growth temperature. In the ZnO film, the substrate temperature may be dominant factor rather than the ion beam irradiation [27]. Fig. 7 show the electromechanical coupling and polarity direction vs substrate temperature in the ZnO films grown by off-axis geometry RF magnetron sputtering [27]. The electromechanical coupling coefficients were determined by using HBAR resonator conversion loss method [28]. As can be seen, the polarity direction of ZnO can be controlled by substrate temperature.

B. *Polarization inverted four layer ZnO film resonator*

By using this polarization control technique, polarization inverted four layer ZnO resonator, (0001)ZnO/SiO_2/(000-1)ZnO/SiO_2/(0001)ZnO/SiO_2/(000-1)ZnO/(0001)Ti/silica glass substrate, were fabricated. Thickness of the ZnO layers were adjusted to within 1.6–1.9 μm. Electromechanical coupling coefficient k_t of each layer were measured to be 0.18–0.21. Thin SiO_2 buffer layers (70–80 nm) were inserted between the O-polar ZnO layer and Zn-polar ZnO layers.

Fig. 8 shows frequency response of the conversion loss of the four layered ZnO high overtone mode bulk acoustic resonator (HBAR). 4th mode resonance excitation with suppression of the 1st, 2nd, and 3rd resonance modes, indicating complete polarization inversion in each layer, were clearly observed.

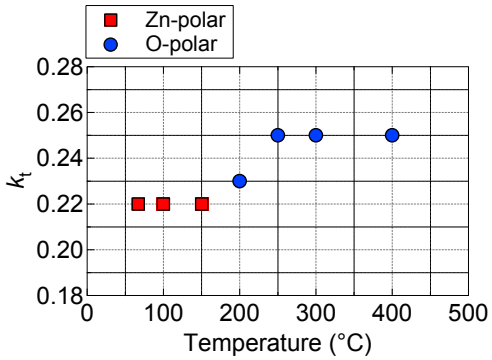

Fig. 7. Electromechanical coupling coefficients and polarity direction of ZnO films grown in differeint substrate temperatures.

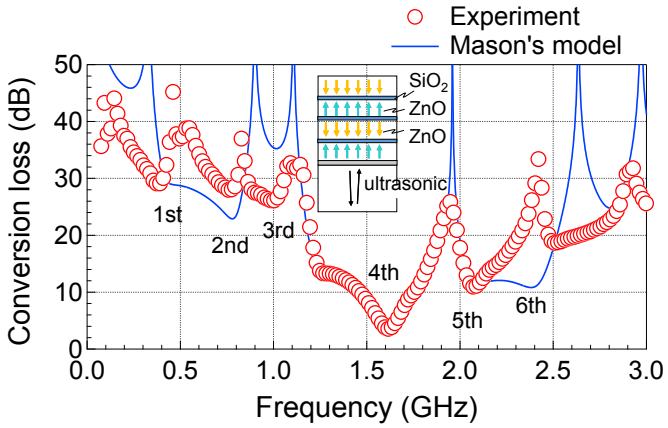

Fig. 8. Frequency response of the conversion loss of the four layered ZnO HBAR, (0001)ZnO/SiO_2/(000-1)ZnO/SiO_2/(0001)ZnO/SiO_2/(000-1)ZnO/(0001)Ti/silica glass substrate.

IV. Enhancement of k_{t2} in New YbAlN Materials

In 2014, we reported the enhancement of k_t^2 in the YbGaN in the GHz range [29]. We also found high k_t^2 of 11% in the YbAlN films in 2015 [3]. After that, in this spring, a replication study by Akiyama confirmed the large piezoelectric constant in the YbAlN [30]. k_t^2 were extracted using the HBAR conversion loss method in the 0.5-1 GHz [29]. Figure 9 shows typical experimental and conversion loss curve of the $Yb_xAl_{1-x}N$ film HBAR resonators. Also shown is a theoretical conversion loss curve simulated by Mason's equivalent circuit model.

Figure 10 the relationship between Yb atomic concentration and k_t^2. We can see apparent increase of k_t^2 of the films. Rocking curve FWHM determined by XRD were also shown.

The theoretical prediction of electromechanical coupling coefficient k_{33}^2 in wurtzite AlN with the addition of Yb were also carried out, based on the density functional theory (DFT) calculations by using the projector augmented-wave (PAW) method [31,32] and the generalized gradient approximation (GGA) with the Perdew-Burke-Ernzerhof (PBE) functional [33] as implemented in the VASP code. The special quasirandom structure (SQS) method was used to model the

random distribution of Yb in AlN structure.[34,35]. A 3×3×2 supercell was used to relax the structure, and to calculate piezoelectric coefficients elastic constants with a 3×3×3 Monkhorst−Pack *k*-mesh, and the plane wave cutoff energy was set to 600 eV. The geometry structures were allowed to be fully relaxed with a convergence criterion of 10^{-9} eV in energy.

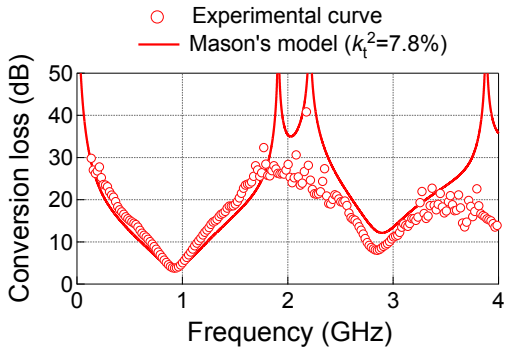

Fig. 9. Typical experimental conversion loss curve of the $Yb_xAl_{1-x}N$ film HBAR resonators. Also shown is a theoretical conversion loss curve simulated by Mason's equivalent circuit model.

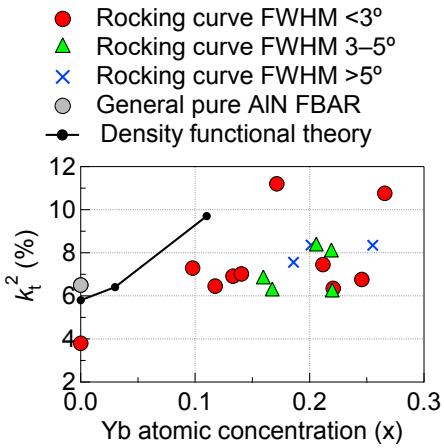

Fig. 10. A relationship between Yb concentrations (x) and k_t^2 in the $Yb_xAl_{1-x}N$. of the film were extracted using HBAR conversion loss method. Also described as black plots are the theoretical prediction obtained by using density fuctional theory.

Figure 11 shows an example of the resonant characteristics of YbAlN SMR. These new wurtzite nitride piezoelectric materials are promising for lead-free high performance ultrasonic devices.

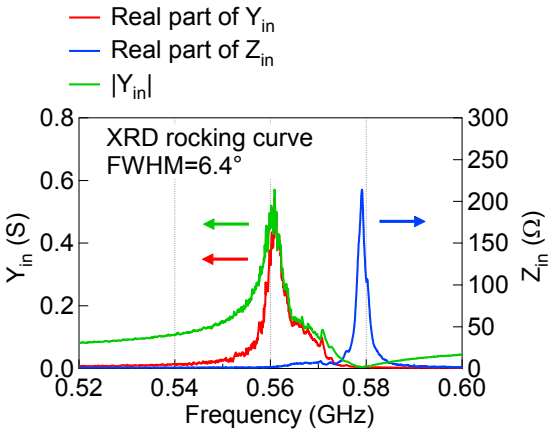

Fig. 11. An example of the resonant characteristics of YbAlN SMR. k_{eff}^2 is 7.8% (which is higher than standard AlN FBAR k_{eff}^2 =6.4%)

V. Conclusions

We showed the methods to obtain polarization inverted multilayer structure in the ScAlN, AlN, ZnO and epitaxial $PbTiO_3$ films. By using slight ion beam irradiation in (perhaps less than 200 eV) the condition of the low substrate temperature during the sputtering film growth, c-axis normal oriented and polarization inverted structure can be obtained in ScAlN, AlN, ZnO films.

On the other hand, the c-axis parallel oriented film growth is induced by high energy ion beam irradiation (for example 3 keV). Moreover, in-plane polarization direction can be easily inverted by 180º rotating ion beam direction. This c-axis parallel and in-plane inverted multilayer structure were obtained for the ZnO and AlN films.

We demonstrated thickness extensional or shear overtone mode resonance excitation by using polarization normal or parallel inverted film resonator, respectively. In addition, frequency switchable resonators were fabricated by using polarization direction switchable epitaxial $PbTiO_3$ films.

These unique polarization inverted structures are expected to open new application in the area of acoustic and optics devices.

References

[1] M. Akiyama, T. Kamohara, K. Kano, A. Teshigahara, Y. Takeushi, N. Kawahara, "Enhancement of piezoelectric response in scandium aluminum nitride alloy thin films prepared by dual reactive cosputtering,", Adv. Mater. Vol. 21, no. 5 pp 593–596, Feb.2008.

[2] T. Yanagitani, K. Arakawa, K. Kano, A. Teshigahara, M. Akiyama,"Giant shear mode electromechanical coupling coefficient k_{15} in c-axis tilted ScAlN films" Proc. IEEE Ultrason. Symp. pp. 2095-2098, (2010).

[3] T. Yanagitani and T. Shimidzu, *US Patent Application* 20190089325.

[4] H. Tanaka, H. Shimizu, and K. Yamada, "Methods for energy trapping of thickness extensional mode and thickness shear mode in piezoelectric ceramic plate," IEICE Trans. Fundamentals (Japanese Edition), vol. 62-A, no. 8, pp 477-484, Aug. 1979.

[5] T. Yanagitani, H. Ichihashi, M. Suzuki, S. Takayanagi, M. Matsukawa, "Elastic constant c_{ij}^E tensors of (0001) $Sc_xAl_{1-x}N$ films (x=0-0.63)," presented

in 2015 IEEE Ultrason. Symp., *Abstract book* 6G-4, p. 326, Oct. 2015.

[6] T. Kittaka, A. Ando, T. Okada, and Y. Sakabe, "Energy trapping of second harmonic of TE mode in piezoelectric ceramic plate," IEICE Technical Report, vol. 87, no. 177, pp. 1-8, Sep. 1987 (in Japanese)

[7] K. Nakamura, H. Ando, and H. Shimizu, "Partial domain inversion in $LiNbO_3$ plates and its applications to piezoelectric devices," Proc. IEEE Ultrason. Symp., pp. 719 − 722, Nov. 1986.

[8] J. D. Larson Ш, S. Mishin, and S. Bader, "Characterization of reversed c-axis AlN thin films," in Proc. IEEE Ultrason. Symp., pp. 1054 − 1059, Oct. 2010.

[9] Y. Fujii, S. Yoshida, S. Misawa, S. Maekawa, and T. Sakudo, "Nonlinear optical susceptibilities of AlN film," Appl. Phys. Lett., vol. 31, pp. 815 − 816, Oct. 1977.

[10] D. N. Nikogosyan, Properties of optical and laser-related materials A Handbook, (John Wiley & Sons, Chichster, 1998).

[11] A. Chowdhury, H. M. Ng, M. Bhardwaj, and N. G. Weimann, "Second-harmonic generation in periodically poled GaN," Appl. Phys. Lett., vol. 83, pp. 1077 − 1079, Aug. 2003.

[12] J. S. Park, T. Minegishi, S. H. Lee, I. H. Im, S. H. Park, T. Hanada, T. Goto, M. W. Cho, T. Yao, S. K. Hong, and J. H. Chang, "Effects of interfacial layer structures on crystal structural properties of ZnO films," J. Vac. Sci. Technol. A, vol. 26, pp. 90 − 96, Feb. 2008.

[13] J. Park, Y. Yamazaki, M. Iwanaga, S. Ahn, H. Jeon, T. Fujiwara and T. Yao, "Second harmonic generation in periodically polarity-inverted zinc oxide," Optics. Express, vol. 18, pp. 7851 − 7856, Apr. 2010.

[14] U. Neumann, R. Grunwald, U. Griebner, G. Steinmeyer, M. Schmidbauer, and W. Seeber, "Second-harmonic performance of a-axis-oriented ZnO nanolayers on sapphire substrates," Appl. Phys. Lett., vol. 87, 171108, Oct. 2005.

[15] M. Stutzmann, O. Ambacher, M. Eickhoff, U. Karrer, A. L. Pimenta, R. Neuberger, J. Schalwig, R. Dimitrov, P. J. Schuck, and R. D. Grober., "Playing with Polarity," Phys. Stat. Sol. (b), vol. 228, pp. 505 − 512, Nov. 2001.

[16] E. Milyutin, S. Harada, D. Martin, J. F. Carlin, N. Grandjean, V. Savu, O. Vaszquez-Mena, J. Brugger, and P. Muralt, "Sputtering of (001)AlN thin films: Control of polarity by a seed layer," J. Vac. Sci. Technol. B, vol. 28, pp. L61 − L63, Nov. 2010.

[17] M. Akiyama, T. Kamohara, K. Kano, A. Teshigahara, and N. Kawahara, "Influence of oxygen concentration in sputtering gas on piezoelectric response of aluminum nitride thin films," Appl. Phys. Lett., vol. 93, 021903, July 2008.

[18] M. Akiyama, T. Kamohara, N. Ueno, and M. Sakamoto, "Polarity inversion in aluminum nitride thin films under high sputtering power," Appl. Phys. Lett., vol. 90, 151910, Apr. 2007.

[19] R. Di Felice and J. E. Northrup, "Energetics of AlN thin films on the Al2O3 (0001) surface," Appl. Phys. Lett., vio. 73, pp. 936 − 938, June 1998.

[20] T. Yanagitani and M. Kiuchi, "Control of in-plane and out-of-plane texture in shear mode piezoelectric ZnO films by ion-beam irradiation," J. Appl. Phys., vol. 102, 044115, Aug. 2007.

[21] S. Takayanagi, T. Yanagitani, and M. Matsukawa, "Unusual growth of polycrystalline oxide film induced by negative ion bombardment in the capacitively coupled plasma deposition," Appl. Phys. Lett., vol. 101, 232902, Dec. 2012.

[22] S. Takayanagi, T. Yanagitani, and M. Matsukawa, "Fabrication of c-axis parallel oriented AlN and ScAlN films by RF bias sputtering," presented at the 2012 IEEE Int. Ultrasonics Symp., Dresden, Germany, Oct. 7-10, 2012.

[23] J. F. Rosenbaum, Bulk Acoustic Wave Theory and Devices (Artech House, Boston, 1988).

[24] M. Suzuki, T. Yanagitani, and H. Odagawa, "Polarity-inverted ScAlN film growth by ion beam irradiation and application to overtone acoustic wave (000-1)/(0001) film resonators" Appl. Phys. Lett., vol. 104, 172905 May 2014.

[25] M. Suzuki, and T. Yanagitani, "RF bias induced polarity inversion of ScAlN film for overtone mode BAW resonator," *Abstract book* 5I-5, p. 511, Sep. 2014.

[26] M. Caro, S. Zhang, T. Riekkinen, M. Ylilammi, M. Moram, O. Lopez-Acevedo, J. Molarius, and T. Laurila "Piezoelectric coefficients and spontaneous polarization of ScAlN," J. Phys.: Condens. Matter, vol. 27, 245901, 2015.

[27] R. Hashimoto, T. Yanagitani, R. Ikoma, S. Takayanagi, M. Suzuki, H. Odagawa, and M. Matsukawa, "Polarity control of c-axis oriented ZnO films and application to polarity-inverted ZnO multilayer resonators," presented in 2015 IEEE Ultrason. Symp., *Abstract book* IUS3-H-6, July 2013.

[28] T. Yanagitani, M. Kiuchi, M. Matsukawa, and Y. Watanabe, "Shear-mode electromechanical coupling coefficient k_{15} and crystallites alignment of (11-20) textured ZnO films," J. Appl. Phys., vol. 102, no. 2, 024110, July 2007.

[29] T. Yanagitani, and M. Suzuki, "Enhanced piezoelectricity in YbGaN films near phase boundary," Appl. Phys. Lett., vol. 104 no. 23, pp. 082911-1 − 082911-4 (2014).

[30] Y. Amano, M. Uehara, S. A. Anggraini, K. Hirata, H. Yamada, M. Akiyama, "Improvement of piezoelectric properties in AlN thin film by Yb addition," *JSAP Spring Meeting* 10a-PA4-8, (2019).

[31] P. E. Blöchl, "Projector augmented-wave method," Phys. Rev. B Vol. 50, pp. 17953 − 17979, Dec. 1994.

[32] G. Kresse and D. Joubert, "From ultrasoft pseudopotentials to the projector augmented-wave method," Phys. Rev. B Vol. 59, pp. 1758 − 1775 Jan. 1999

[33] J. P. Perdew, K. Burk, M. Ernzerho, "Generalized Gradient approximation made simple" Phys. Rev. Lett., Vol. 77, 3865−3868 Oct. 1996

[34] A. Zunger, S. Wei, L. Ferreira, and J. Bernard, "Special quasirandom structures," Phys. Rev. Lett., Vol. 65, pp. 353 July 1990.

[35] A.V.Ruban and I. A. Abrikosov, "Configurational thermodynamics of alloys from first principles: effective cluster interactions," Rep. Prog. Phys.,Vol. 71, 046501 Mar. 2008.